

soya, J. Low Temp. Phys. 27, 245 (1977).

¹⁴S. D. Bader, G. S. Knapp, S. K. Sinha, P. Schweiß, and B. Renker, Phys. Rev. Lett. 37, 344 (1976); S. D. Bader, S. K. Sinha, and R. N. Shelton, in *Superconduct-*

tivity in d- and f-Band Metals, edited by D. H. Douglass (Plenum, New York, 1976), p. 209.

¹⁵D. Rainer, to be published.

¹⁶G. Bergmann and D. Rainer, Z. Phys. 263, 59 (1973).

Phase Diagrams of Pseudo One-Dimensional Heisenberg Systems

J. P. A. M. Hijmans, K. Kopinga, F. Boersma, and W. J. M. de Jonge

Department of Physics, Eindhoven University of Technology, Eindhoven, The Netherlands

(Received 13 January 1978)

We present the first theoretical results on the anomalous field dependence of the Néel temperature for a system of loosely coupled classical Heisenberg chains with orthorhombic anisotropy for different directions of the applied magnetic field. The results compare favorably with the experimental phase diagrams of a series of selected $S = \frac{5}{2}$ compounds with varying degrees of one dimensionality and anisotropy.

The ordering temperature $T_N(H)$ of a pseudo one-dimensional Heisenberg antiferromagnet may increase drastically when an external magnetic field is applied. This initially surprising effect has been documented recently by a number of experimental results.¹⁻⁵ It seems that the theoretical approach suggested by Villain and Loveluck,⁶ which is based on the behavior of the correlation length within the individual chains in the classical spin model,⁷⁻¹⁰ gives at least the right order of magnitude. However, as we will show, the drastic influence of some anisotropy resulting in essentially different phase boundaries with the field applied along different directions (including the introduction of a spin-flop phase) cannot be reproduced by this isotropic theory. Therefore a conclusion about the validity of the description of this effect is precluded so far.

In this Letter we will present the first results of a transfer-matrix approach for the classical Heisenberg chain with small orthorhombic anisotropy. We will show that this approach is capable of reproducing the field dependence of the Néel temperature in a series of real pseudo one-dimensional Heisenberg $S = \frac{5}{2}$ systems with the field along each of the three principal axes.

In Figs. 1-3 our data on the phase diagrams are presented for a selected, representative series of pseudo one-dimensional systems. Some characteristic parameter values of this series are tabulated in Table I. The data were obtained from a continuous heating method, thus identifying the transitions by the maxima in the specific heat. From inspection of these results it is obvious that in a general sense the rise in $T_N(H)$

strongly depends on the degree of one dimensionality, characterized by the entities in Table I. This indicates that basically the understanding of this anomalous behavior must be sought in the properties of the individual chains. Therefore, we will treat the system as consisting of loosely coupled chains.

For such a system T_N is implicitly given in the mean-field approach by⁵

$$2zJ'\chi(T_N(H), H) = 1, \quad (1)$$

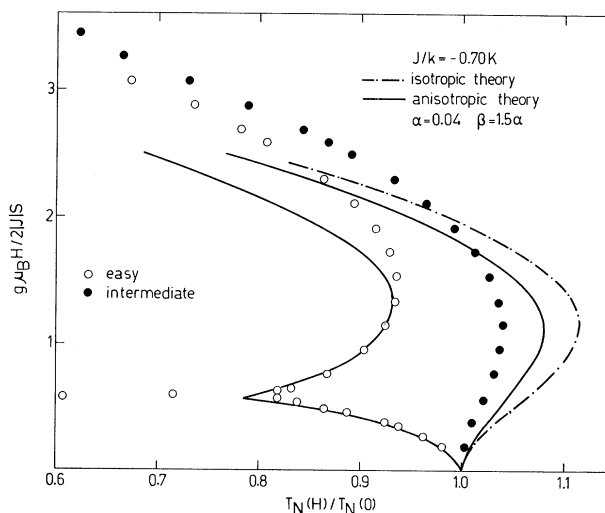


FIG. 1. Experimental phase diagram of $(\text{NC}_5\text{H}_6)\text{MnCl}_3 \cdot \text{H}_2\text{O}$ (PMC), together with the theoretical predictions. Data for the hard axis are not shown since they reveal a more complicated phase diagram which is most likely due to a small canting of the magnetic moments.

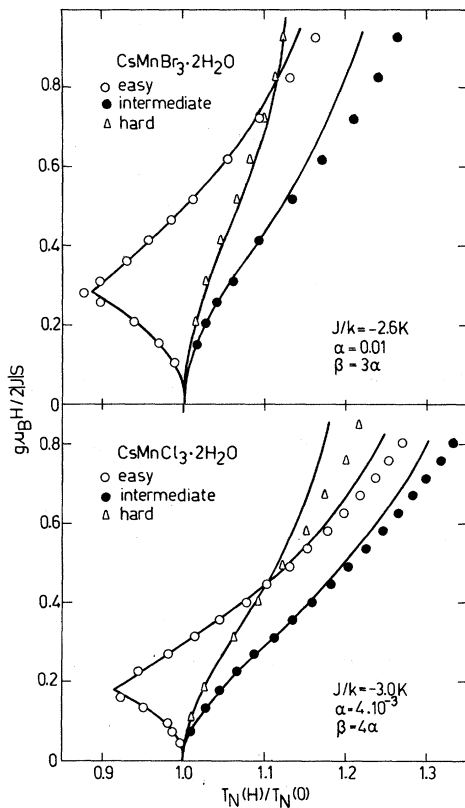


FIG. 2. Phase diagram of $\text{CsMnBr}_3 \cdot 2\text{H}_2\text{O}$ (CMB) and $\text{CsMnCl}_3 \cdot 2\text{H}_2\text{O}$ (CMC). The drawn curves denote the theoretical prediction in the presence of orthorhombic anisotropy. The theoretical results for the isotropic case are not plotted separately, since they almost coincide with the predicted behavior for the intermediate axis.

where χ is the staggered susceptibility of an isolated chain and zJ' is interchain interaction. Hence we will have to evaluate the staggered susceptibility, $\chi(T, H)$, of an isolated chain with or-

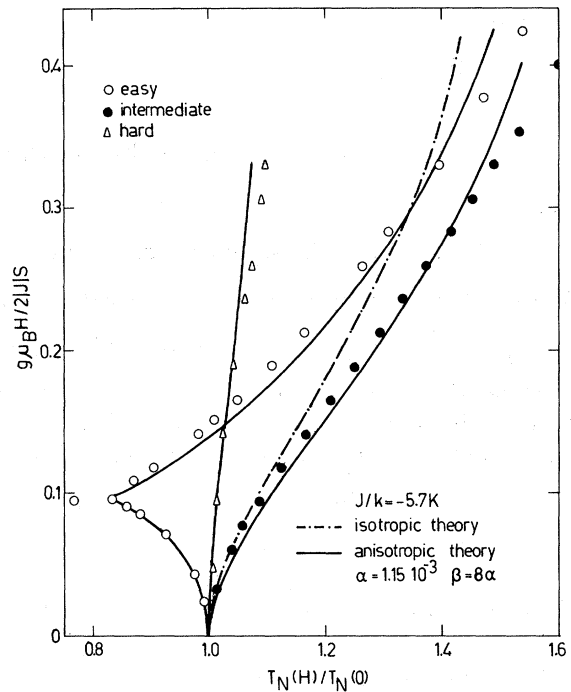


FIG. 3. Experimental phase diagram of $(\text{CH}_3)_2\text{NH}_2 \times \text{MnCl}_3$ (DMMC), together with the theoretical predictions.

thorhombic anisotropy. We will not apply the usual approximation of χ in terms of the correlation length.^{6,16} As we are dealing with high-spin ($S = \frac{5}{2}$) systems we will evaluate χ in the framework of the classical spin model. Moreover, it has previously been shown that the classical model gives remarkably good results for those thermodynamic variables in the paramagnetic state which greatly depend on long-range correlation.^{17,18}

We will consider here the classical nearest-neighbor Hamiltonian of orthorhombic symmetry,

TABLE I. Review of some characteristic parameters of the compounds studied in this Letter. $T_N(0)$ is the zero-field ordering temperature; J and J' are the intrachain and interchain exchange coupling, respectively; and S_{crit} denotes the entropy ratio $S(T_N)/S(\infty)$. The anisotropy parameters α and β are defined in the text.

Compound	$T_N(0)$ (K)	J/k (K)	S_{crit}	J'/J	α	β/α	Ref.
$(\text{NC}_5\text{H}_8)\text{MnCl}_3 \cdot \text{H}_2\text{O}$	2.38	-0.7	39%	7×10^{-2}	4×10^{-2}	1.5	11
$\text{CsMnBr}_3 \cdot 2\text{H}_2\text{O}$	5.75	-2.6	15%	10^{-2}	1×10^{-2}	3	12, 13
$\text{CsMnCl}_3 \cdot 2\text{H}_2\text{O}$	4.89	-3.0	12%	8×10^{-3}	4×10^{-3}	4	13
$(\text{CH}_3)_2\text{NH}_2\text{MnCl}_3$	3.60	-5.8	3%	10^{-3}	1.15×10^{-3}	8	14

given by

$$\mathcal{H}_{\text{chain}}(\mathfrak{S}_i, \mathfrak{S}_{i+1}) = \sum_{i=-\infty}^{+\infty} \left\{ \frac{1}{2} g_B HS(S_i^z + S_{i+1}^z) + 2JS(S+1)[\mathfrak{S}_i \cdot \mathfrak{S}_{i+1} + \delta(S_i^x S_{i+1}^x - \frac{1}{3} \mathfrak{S}_i \cdot \mathfrak{S}_{i+1}) + \epsilon(S_i^x S_{i+1}^x - S_i^y S_{i+1}^y)] \right\}, \quad (2)$$

where

$$S_i = (S_i^x, S_i^y, S_i^z) = (\cos\varphi_i \sin\theta_i, \sin\varphi_i \sin\theta_i, \cos\theta_i). \quad (3)$$

The central problem in the transfer-matrix approach is to solve the integral equation

$$\int_0^\pi d\theta_2 \int_0^{2\pi} d\varphi_2 \sin\theta_2 \exp[-\mathcal{H}(\mathfrak{S}_1, \mathfrak{S}_2)/kT] \psi(\theta_2, \varphi_2) = \lambda \psi(\theta_1, \varphi_1) \quad (4)$$

because all static properties of the chain can be formulated in terms of the eigenvalues and eigenfunctions of this equation.

In order to reduce the number of integration variables in Eq. (4) we introduce the Fourier expansions

$$\psi(\theta_i, \varphi_i) = (2\pi \sin\theta_i)^{-1/2} \sum_{m=-\infty}^{+\infty} \Phi_m(\theta_i) \exp(im\varphi_i) \quad (5)$$

and

$$\exp[-\mathcal{H}(\mathfrak{S}_1, \mathfrak{S}_2)/kT] = (2\pi)^{-1} \sum_{m=-\infty}^{+\infty} \sum_{l=-\infty}^{+\infty} K_{ml}(\theta_1, \theta_2) \exp[i(m\varphi_1 - l\varphi_2)]. \quad (6)$$

Substitution of Eqs. (5) and (6) in Eq. (4) yields [because of the orthogonality of the functions $\exp(im\varphi_i)$] the set of coupled integral equations

$$\sum_{l=-\infty}^{+\infty} \int_0^\pi d\theta_2 (\sin\theta_1 \sin\theta_2)^{1/2} K_{m,l}(\theta_1, \theta_2) \Phi_l(\theta_2) = \lambda \Phi_m(\theta_1), \quad m=0, \pm 1, \pm 2, \dots \quad (7)$$

It will be clear that Eq. (7) cannot be handled numerically unless the infinite summation is truncated in some way. In the case of axial symmetry around the field direction⁸⁻¹⁰ this gives no complications because $K_{m,l}(\theta_1, \theta_2) \sim \delta_{m,l} K_{m,m}(\theta_1, \theta_2)$, and only one term in the summation survives.

If the deviations from axial symmetry are small, that is $|2JS(S+1)\epsilon| \ll kT$, a meaningful truncation is possible because one finds a rapid decrease in magnitude of the $K_{m,l}(\theta_1, \theta_2)$ with increasing $|m-l|$. Moreover, only a restricted number of equations has to be retained because the susceptibilities depend mainly on the perturbed eigenstates related to $m=0, \pm 1$ in the axially symmetric case. Even after this truncation, practical calculations are almost impossible without further simplifications. However, exploiting the C_{2v} symmetry of the system, Eq. (7) can be factorized into four smaller subsets. The integrals over θ_2 occurring in each of these subsets are approximated by a discrete quadrature scheme. The choice of a set of values for θ_1 identical to the abscissas used in the integration over θ_2 results in a matrix eigenvalue equation⁸ which can be diagonalized by standard routines. The dimension of these matrices, which ultimately sets a limit to the applicability of the method, increases progressively when $|J|/kT$ increases

because both the number of coupled equations and the number of abscissas needed to obtain results of sufficient accuracy grow rapidly at lower temperatures.

Using the method sketched above, we calculated phase diagrams for $(\text{NC}_5\text{H}_6)\text{MnCl}_3 \cdot \text{H}_2\text{O}$ (PMC), $\text{CsMnBr}_3 \cdot 2\text{H}_2\text{O}$ (CMB), $\text{CsMnCl}_3 \cdot 2\text{H}_2\text{O}$ (CMC), and $(\text{CH}_3)_2\text{NH}_2\text{MnCl}_3$ (DMMC). In order to eliminate the interchain molecular-field constant zJ' , Eq. (1) was applied in the form $\chi(T_N(H), H) = \chi(T_N(0), 0)$, where χ is the appropriate staggered susceptibility. Basically we did not use adjustable parameters; the values for J were fixed to the reported values. From the zero-field energy differences, per spin, between the antiferromagnetically aligned states parallel to the easy and intermediate axis (ΔE_1) and the easy and hard axis (ΔE_2) we define the reduced anisotropy energies α and β as

$$\alpha = \Delta E_1/2|J|S(S+1), \quad \beta = \Delta E_2/2|J|S(S+1). \quad (8)$$

Note that the values of ϵ and δ for given α and β depend upon the correspondence between the coordinate system x, y, z and the magnetic axes. For CMC and CMB, α and β were taken from the literature,^{12,13} whereas for PMC and DMMC the anisotropy parameters were obtained in an analo-

gous way, as will be reported elsewhere.¹⁹ Theoretical phase diagrams obtained with quadratic single-ion anisotropy instead of Eq. (2) showed only minor deviations from the results presented in Figs. 1-3.

With the field applied along the easy axis, we have to consider two different susceptibilities corresponding to the directions of the staggered field in the antiferromagnetic and spin-flop state. The phase boundaries found in this way intersect at the bicritical field H_{bic} which is given to a very good approximation by $g\mu_B H_{\text{bic}} = 4|J|S\sqrt{2}\alpha$. For fields higher than H_{bic} the spin-flop phase yields the highest, and thus physically realized, value of $T_N(H)$, while for fields smaller than H_{bic} the situation is reversed.

The agreement between experimental and theoretical results is satisfying but it deteriorates somewhat at higher values of the reduced field $g\mu_B H/2|J|S$. Whether this is due to a deficiency in the applicability of Eq. (1) at high fields remains to be seen. Possibly a self-consistent type of approach would give better results. However, these high-field deviations could also be due to the suppression of quantum fluctuations, as described by Imry, Pincus, and Scalapino.¹⁶ Therefore it seems worthwhile to investigate the effect of quantum corrections on the present theory. The results of the present analysis may be summarized by stating that the, at first sight, anomalous behavior of the phase boundaries of pseudo one-dimensional Heisenberg systems can be quantitatively understood from the behavior of the staggered susceptibilities of the isolated chains, provided that the orthorhombic anisotropy terms are not neglected.

The authors wish to acknowledge the assistance of J. C. Schouten, J. Millenaar, and J. A. M. Roos. This research is partially supported by

the Stichting Fundamenteel Onderzoek der Materie.

¹D. P. Almond and J. A. Rayne, *Phys. Lett.* **55A**, 137 (1975).

²W. G. Clark, L. J. Azvedo, and E. O. McLean in *Proceedings of the Fourteenth International Conference on Low Temperature Physics, Otaniemi, Finland, 1975* (North-Holland, Amsterdam, 1975), p. 391.

³C. Dupas and J. P. Renard, *Solid State Commun.* **20**, 381 (1976).

⁴J. P. Goren, T. O. Klaassen, and N. J. Poulis, *Phys. Lett.* **62A**, 453 (1977).

⁵W. J. M. de Jonge, J. P. A. M. Hijmans, F. Boersma, J. C. Schouten, and K. Kopinga, *Phys. Rev. B* (to be published).

⁶J. Villain and J. M. Loveluck, *J. Phys. (Paris)*, *Let.* **38**, L77 (1977).

⁷M. E. Fisher, *Am. J. Phys.* **32**, 343 (1964).

⁸M. Blume, P. Heller, and N. A. Lurie, *Phys. Rev. B* **11**, 4483 (1975).

⁹J. M. Loveluck, S. W. Lovesey, and S. Aubry, *J. Phys. C* **8**, 3841 (1975).

¹⁰S. W. Lovesey and J. M. Loveluck, *J. Phys. C* **9**, 3639 (1976).

¹¹P. M. Richards, R. K. Quinn, and B. Morosin, *J. Chem. Phys.* **59**, 4474 (1973).

¹²T. Iwashita and N. Uryû, *J. Phys. Soc. Jpn.* **39**, 1226 (1975).

¹³See, for instance, K. Kopinga, *Phys. Rev. B* **16**, 427 (1977), and references therein.

¹⁴R. D. Caputo and R. D. Willett, *Phys. Rev. B* **13**, 3956 (1976).

¹⁵See, for instance, Y. Imry, *Phys. Rev. B* **13**, 3018 (1976), and references therein.

¹⁶Y. Imry, P. Pincus, and D. Scalapino, *Phys. Rev. B* **12**, 1978 (1975).

¹⁷R. J. Birgeneau, R. Dingle, M. T. Hutchings, G. Shirane, and S. L. Holt, *Phys. Rev. Lett.* **26**, 718 (1971).

¹⁸S. A. Scales and H. A. Gersch, *Phys. Rev. Lett.* **28**, 917 (1972).

¹⁹K. Takeda, J. C. Schouten, K. Kopinga, and W. J. M. de Jonge, *Phys. Rev. B* **17**, 1285 (1978).